MAGMA (2005) 18: 144–161
DOI 10.1007/s10334-005-0107-7

RESEARCH ARTICLE

N. W. Lutz
S. E. Franks
M. H. Frank
S. Pomer
W. E. Hull

Investigation of multidrug resistance in cultured human renal cell carcinoma cells by ^{31}P-NMR spectroscopy and treatment survival assays

Received: 7 February 2005
Revised: 18 April 2005
Accepted: 2 May 2005
Published online: 23 June 2005

N. W. Lutz · S. E. Franks · W. E. Hull
Central Spectroscopy Department,
German Cancer Research Center
(DKFZ), Heidelberg, Germany

M. H. Frank · S. Pomer
Department of Urology,
University of Heidelberg,
Heidelberg, Germany

M. H. Frank
Renal Division, Dept. of Medicine,
Brigham and Women's Hospital,
Boston, MA, USA

N. W. Lutz (✉)
Université Louis Pasteur,
Faculté de Médecine, Institut Physique
Biologique,
4 rue Kirschleger, F-67000,
Strasbourg, France
E-mail: Lutz@ipb.u-strasbg.fr
Tel.: +33-390244047
Fax: +33-390244084

Abstract KTCTL-26 and KTCTL-2 are renal cell carcinoma (RCC) lines with high and low expression of P-170 glycoprotein, respectively. Inherent differences between the two cell lines in terms of phosphate metabolites and growth characteristics in culture were examined for possible association with multidrug resistance (MDR). Differences in response to drug treatment were investigated for 40 h incubations with various doses of vinblastine (VBL) alone or as cotreatments with various concentrations of the calcium antagonist diltiazem (DIL) and/or interferon−α (IFN-α). Treatment effects were quantitated using the MTT survival assay and ^{31}P magnetic resonance spectroscopy (MRS) to determine phosphate metabolite profiles in intact cells. KTCTL-2 and KTCTL-26 cells exhibited significant inherent differences in phosphocholine, glycerophosphocholine, glycerophosphoethanolamine, and phosphocreatine levels. KTCTL-26 cells were more sensitive than KTCTL-2 to 0.011 μM VBL alone (87% vs. 102% survival) or to 0.011 μM VBL + 10 μM DIL (55% vs. 80% survival). The latter treatment resulted in a significant decrease in the ratio of phosphocholine to glycerophosphocholine in KTCTL-26 cells but no significant changes in phosphate metabolites in KTCTL-2 cells. Metabolomic ^{31}P MRS detects different metabolite profiles for RCC cell lines with different MDR phenotypes and may be useful for noninvasive characterization of tumors in a clinical setting.

Keywords Renal cell carcinoma · P-glycoprotein · Multidrug resistance · ^{31}P-NMR spectroscopy · Metabolomics

Abbreviations DIL: Diltiazem · FCS: Fetal calf serum · GPC: Glycerophosphocholine · GPE: Glycerophosphoethanolamine · IFN: Interferon · IL-2: Interleukin-2 · MDP: Methylene diphosphonate · MDR: Multidrug resistance · MRP1: Multidrug resistance-associated protein · MTT: 3-[4,5-dimethylthiazol-2-yl]-2,5-diphenyltetrazolium bromide · NDP: All nucleoside 5′-diphosphates · NDP-Hex: All nucleoside 5′-diphospho-1-hexoses · NTP: All nucleoside 5′-triphosphates · PC: Phosphocholine · PCr: Phosphocreatine · PDE: Phosphodiester · PE: Phosphoethanolamine · P-gp: P-glycoprotein · P_i: Inorganic phosphate · PME: Phosphomonoester · P-170: P-170 glycoprotein · RCC: Renal cell carcinoma · RPMI 1640: Roswell Park Memorial Institute medium number 1640 · TNF: Tumor necrosis factor · VBL: Vinblastine.

Introduction

Renal cancer accounts for 2–3% of all adult cancers [1]. The treatment of renal cell carcinomas (RCC), in particular *metastatic* RCC, presents a major problem since all of the therapeutic options available to date have shown only very low success rates [2]. Human RCC displays a high degree of intrinsic drug resistance, and patient response to chemotherapeutic treatment is poor [3,4]. Increased expression of the membrane-associated P-170 glycoprotein, a product of the *mdr1* gene, has been associated with the multidrug-resistant phenotype [5–7], and there is evidence that P-170 (MDR1) acts primarily as an ATP-dependent pump which exports drug molecules across the cellular membrane [8]. Therefore, resistance which is associated with a P-glycoprotein such as P-170 is characterized by a decrease in intracellular accumulation and retention of drug [6,9,10]. Chemosensitizers such as calcium antagonists can partially reverse drug resistance by interfering with the pump mechanism, resulting in increased intracellular drug accumulation [11–13] (for an overview of drugs currently used for MDR reversal, see Silverman [14]). The propensity of *renal* cancers to develop the *mdr1*-expressing genotype is probably related to the important function of the kidney in clearing xenobiotics, for which the P-glycoprotein pump may play an essential role. The MDR1 protein is expressed in mesangial cells and in proximal tubule cells [15], which are involved in blood filtration and in reabsorption (Na^+, glucose, amino acid, phosphate), respectively. For a different class of P-glycoproteins, produced by the *mdr3* gene (also called *mdr2*), a "flippase" model has been proposed to explain the mechanism by which specific membrane phospholipids and bound or intercalated substrates (e.g. cytotoxic drugs) are translocated from the inner to the outer membrane leaflet [16, 17]. Despite more than 20 years of effort and numerous clinical trials, many fundamental questions remain to be answered before modulation of multidrug resistance can become an effective clinical tool [18].

^{31}P nuclear magnetic resonance spectroscopy (NMR or MRS) allows the quantitative analysis of phosphate metabolites in intact cancer cells and, thus, provides information concerning key components of energy and phospholipid metabolism [19]. ^{31}P-MRS has been used to demonstrate that transfection of various cancer cell lines with the *mdr1* gene, encoding for P-170 (MDR1), results in altered levels of phosphomonoesters (PME) and phosphodiesters (PDE) and an increase in phosphocreatine (PCr) and ATP levels in comparison with wild-type cells [20]. Over the past decade ^{31}P-, ^{1}H- and ^{13}C- MRS studies of a variety of cancer cell lines have revealed further differences in energy and lipid metabolism when comparing drug-sensitive parental cells with variants rendered multidrug-resistant by selection for drug tolerance [20–26]. Little is known, however, about the functional significance of the metabolic characteristics exhibited by MDR1-expressing cells.

We present here a study of two human RCC lines, established in the Tumor Bank of the German Cancer Research Center, which differ with regard to growth characteristics, degree of differentiation, expression of P-170, and sensitivity to vinblastine (VBL). With ^{31}P-MRS we examined the phosphate metabolite profiles of the two cell lines under indentical culture conditions before and after drug treatment in order to identify metabolomic patterns which can be associated with the MDR1-associated multidrug resistance phenotype. Our hypothesis is that previously reported P-170 expression-dependent differences in phosphate metabolite profiles may be of functional significance for the MDR mechanism, and particularly, that increased PCr levels may reflect an increased energy requirement of the ATP-dependent transporter. We have also investigated modulation of VBL treatment effects (cell kill, phosphate metabolites) by cotreatment with the calcium antagonist diltiazem (DIL) and/or interferon-α (IFN-α).

Table 1 Characteristics of clear cell RCC cell lines

	KTCTL-2	KTCTL-26
Source	Grade II RCC	Grade II RCC
TNM class	pT3a, N1, MX	pT2, Nx, M1
Doubling time	23 h	35 h
Morphology	Polygonal	Lengthy, irregular
Differentiation	Poor	Higher vs. KTCTL-2
P-170 expression	Low	Mod. high
Growth in culture	Multilayer	Contact inhibition at confluence

Materials and methods

Cells and Culture Conditions

Cell lines

KTCTL-2 and KTCTL-26 are human clear-cell RCC lines which were derived from primary tumor specimens (grade II RCC) surgically resected in the Department of Urology at the University Clinic, Heidelberg, and are maintained as frozen stocks in the Tumor Bank of the German Cancer Research Center (DKFZ), Heidelberg. TNM classification [27] and other properties of these cell lines are summarized in Table 1. Seed stocks were prepared from culture at passage 19 (KTCTL-2) and passage 22 (KTCTL-26), and were stored in liquid nitrogen as suspensions of 2×10^6 cells/ml in RPMI 1640 medium supplemented with 10% fetal calf serum and 10% DMSO as cryoprotectant.

Cell culture

Frozen stocks were thawed and maintained in culture in RPMI 1640 supplemented with 10% fetal calf serum (same batch for both lines), 2 mM glutamine, 100 units/ml penicillin, 100 μg/ml streptomycin, and 10 mM HEPES at pH 7.4. This growth medium was completely replaced every two to three days, and cultures were passaged before confluence at intervals of 1–2 weeks. Cell culture plastics were manufactured by Falcon (Kurt Migge GmbH, Heidelberg, FRG). All cell culture media, sera, and biochemicals were obtained from Biochrom KG (Berlin, FRG), except for the Ringer's saline which was obtained from Fresenius AG (Bad Homburg, FRG).

For growth curve determinations, cells were seeded at 10^4 cells/cm^2 in T25 flasks and medium was replenished daily. Triplicate flasks were harvested daily by trypsinization and counted using a hemocytometer, whereby the standard trypan blue dye exclusion test was used to assay membrane integrity (viability).

Assay of protein expression

The KTCTL-2 and KTCTL-26 cell lines had been previously analyzed semiquantitatively for P-170 glycoprotein expression (E. Pommerenke and M. Volm, personal communication) at the Institute of Experimental Pathology at the German Cancer Research Center, as part of an independent study of a panel of human RCC lines [28]. The immunoassay for P-170 was repeated for the cell stocks used in the present study according to previously published methods, using the P-170-specific monoclonal antibodies C219 and JSB1 obtained from Centocor (Malvern, PA) [29]. The KTCTL-2 and KTCTL-26 lines were characterized as having low and high P-170 expression, respectively.

Concurrent expression of vimentin and cytokeratin 18, a specific marker of renal tissue, was confirmed for both cell lines by immunohistochemical staining according to previously published methods [30] to verify the renal origin of these cell lines. The mouse monoclonal antibodies (Boehringer, Mannheim, FRG) Mab V9 (2 μg/ml), directed against vimentin, and Mab CK2 (10 μg/ml), directed against cytokeratin 18 were used.

MTT assays

The effect of drugs on the survival of RCC lines in culture (Series 1) was quantitated using a modification of the MTT assay for mitochondrial dehydrogenase [31]. MTT (3-[4,5-dimethylthiazol-2-yl]-2,5-diphenyltetrazolium bromide) was obtained from Sigma (Deisenhofen, FRG). We first established that conversion of MTT to the formazan dye under control conditions (no drugs) was proportional to the number of viable cells. Cells were seeded in 35 mm petri dishes at a range of densities (5×10^4 to 10^6 cells per dish), and allowed to settle and attach overnight. On the next day, the medium was replaced with 1 ml of fresh medium containing 0.5 g/ml MTT from a fresh stock solution (5 mg/ml MTT in PBS) prepared just prior to the assay. After a 4 h incubation with MTT, the medium was withdrawn, and each dish was rinsed twice with 1 ml PBS. After the final removal of PBS, the formazan dye was solubilized in 0.5 ml acidic isopropanol (90 vol% isopropanol, 10 vol% 1 N HCl). The cells were exposed to this solvent for 15 min, and the resulting solution was repeatedly flowed over the surface of the cell culture to ensure optimal dissolution of the dye. Subsequently, 0.2 ml aliquots from each Petri dish were transferred to a 96-well plate, and absorbance at 570 nm was read on an ELISA reader. An additional well containing 0.2 ml acidic isopropanol was used as a solvent blank, whose absorbance was automatically subtracted from the values from the other wells by the ELISA reader. Each assay was performed in triplicate and mean values of absorbance were used in the subsequent analysis. The expected linear relationship between dye concentration (optical absorbance) and cell number was obtained (data not shown). The regression line parameters were $r^2 = 0.966$, slope = 5.04×10^{-7} for KTCTL-2 and $r^2 = 0.964$, slope = 9.78×10^{-7} for KTCTL-26.

Treatment protocols

Drugs used

VBL was obtained as vinblastine sulfate (Velbe, MW = 909) from Lilly Deutschland GmbH (Bad Homburg, FRG). The calcium antagonist, diltiazem (DIL), was obtained as diltiazem hydrochloride (Dilzem, MW = 451) from Goedecke GmbH (Freiburg, FRG). Drugs were stored in original bottles at 4°C and protected from light exposure. Immediately prior to use, vials were removed from the refrigerator, and solutions were prepared according to the manufacturer's instructions, with serial dilutions to obtain the desired concentrations in culture medium. Recombinant interferon (IFN)-α2b (Intron A, Essex Pharma, Munich, FRG) was used as previously described [32].

Survival assays (Series 1)

Cells suspended in our standard growth medium were seeded in 35 mm Petri dishes (1 ml per dish) at the desired densities (5.0×10^5 cells/dish for KTCTL-2 and 3.5×10^5 cells/dish for KTCTL-26). These cell numbers resulted in similar absorbance values in the MTT assay for both cell lines under control conditions (see above). Twenty-four hours after seeding, the growth medium was replaced with the desired treatment medium and incubated according to the appropriate protocol (typically 40 h for dose comparisons, see Table 2). In the case of VBL + DIL treatment, cells were preincubated with DIL at the chosen concentration for one hour before addition of VBL. In analogous experiments, cells were treated with 2000 or 10000 U/ml IFN-α2b, with or without co-incubation with DIL and VBL (Table 2).

Phosphate metabolite assays (Series 2)

For NMR experiments, cells were seeded into T175 flasks at 10^4 cells/cm^2 on day 0 (30 ml growth medium per flask).

Table 2 Treatment and control culture media [a]

Series 1 (survival)	DIL (μM) [b]	VBL (μM) [c]	IFN-α(U/ml) [d]
controls	–	–	–
A	0.1, 1.0, 10, 100	–	–
B	–	0.011, 0.11, 1.1, 11.0	–
C	0.1, 1.0, 10, 100	0.011, 0.11, 1.1	–
D	–	–	2000
E	0.1, 1.0, 10	–	2000
F	–	0.011, 0.11, 1.1	2000
G	0.1, 1.0, 10	0.011, 0.11, 1.1	2000
H	–	–	10000
Series 2 (NMR)			
controls	–	–	–
A	10	–	–
B	–	0.011, 1.1	–
C	10	0.011, 1.1	–
D	–	–	10000

[a] The basic control culture medium was RPMI 1640 supplemented as described in the Methods; matched control cultures were prepared for each treatment group shown. The standard incubation time for comparative studies was 40 h; the use of other times is described in the text where appropriate

[b] Diltiazem hydrochloride: 1 μg/ml = 2.22 μM (MW = 451). Typical max. concentration found in blood of DIL-treated patients: 0.44 μM [77]

[c] Vinblastine sulfate: 1 μg/ml = 1.10 μM (MW = 909). Typical max. concentration found in serum of VBL-treated patients: 0.0023 μM [78]

[d] Interferon-α2b. Typical max. serum concentration of IFN-α achieved in renal-cancer patients: 1000 U/ml [79, 80]

Subsequently, medium was changed every second day until subconfluency was reached (typically on day 4 for KTCTL-2 and day 5 for KTCTL-26 cells). At this time, the growth medium was replaced with the desired treatment medium, and the cells were incubated according to the protocol shown in Table 2.

Cell survival analysis

For the experiments of Series 1 cultured cells were treated according to the protocols of Table 2. At the end of drug treatment, medium was aspirated and replaced with 1 ml of growth medium containing 0.5 mg/ml MTT, and the MTT assay was carried out as described above. The absorbance data (A_{mean} for $n = 3$ determinations) for treated cells vs. untreated controls were used to compute survival according to Eq. (1):

$$\% \text{ survival} = [A_{mean}(\text{treated})/A_{mean}(\text{control})] \times 100 \quad (1)$$

Phosphate Metabolite Profiles by ^{31}P NMR

Preparation of cell suspensions

For the experiments of Series 2 cultured cells were treated according to the protocols of Table 2 and prepared as suspensions at 4°C for NMR analysis using methods described previously [33–35]. Briefly, trypsinized cells were washed twice in 25 ml ice-cold Ringer's saline containing 10 mM HEPES to remove culture medium. From the second wash suspension, a 0.25 ml aliquot was removed for cell counting and viability testing using trypan blue dye exclusion. The final cell pellet, typically 2–7 × 10^7 cells, was resuspended in 1 ml Ringer's/HEPES buffer at pH 7.2 and transferred to an 8 mm NMR tube placed inside a 10 mm NMR tube containing a 50:50 mixture of Ringer's/HEPES and D_2O which provided a field/frequency deuterium lock signal.

Preparation of cells for perfusion experiments

Continuous NMR observation of phosphate metabolism over an extended period of time (3–4 days) was performed using a perfusion system for cells embedded in matrigel threads, as described previously [33, 36]. Cells harvested from standard culture, as described above, were mixed with matrigel, extruded as threads, and transferred to a 10 mm NMR tube modified for perfusion with oxygenated control or drug-containing culture medium at 37°C. Sequential ^{31}P NMR spectra (1 h acquisitions) of the metabolically active cells were obtained using the same acquisition parameters as for cell suspensions (see below).

^{31}P NMR data acquisition

Spectra of whole-cell suspensions were obtained at 202.46 MHz (11.7 T) and 4°C on a Bruker AM-500 NMR spectrometer using a 10 mm ^{31}P/^{1}H dual probehead and inverse-gated ^{1}H decoupling to suppress NOE effects. The important data acquisition

parameters were: spectral width = 13158 Hz, 8 K time-domain data points, acquisition time AQ = 0.31 s, 45° excitation pulse (12 μs), WALTZ-16 broadband ^{1}H-decoupling (gated on only during acquisition), repetition time TR = 2 s. A total of 1800 transients (1 h measurement time) was accumulated for each sample. As found previously the levels of ^{31}P metabolites remained relatively stable under these conditions [37].

NMR data processing

Bruker's WIN-NMR software for PCs underMICROSOFT WINDOWS was used for all processing steps. FIDs were multiplied by an exponential window function (line-broadening LB = 8 Hz), zero-filled to 16 K and Fourier transformed. The chemical shift scale was defined by setting glycerophosphocholine (GPC) to 3.06 ppm, which corresponds to phosphocreatine at 0 ppm at pH 7. After phase and baseline correction lineshape fitting by Lorentzian deconvolution was performed, using the minimum number of Lorentzians (17–20) necessary to adequately fit all resolved peaks and the complex regions of overlapping signals corresponding to PME or Pα in nucleotides and Pα,Pβ in NDP-hexoses. The integrals of the fitted resonance lineshapes were corrected for partial saturation and residual NOE, as described earlier [33, 35], by multiplying with the following saturation factors (determined at 4°C): 1.0 for PCr and all nucleotides; 1.05 for GPE, GPC; 1.08 for Glc-6P and triose phosphates in the range 6.9–7.5 ppm; 1.13 for P_i and PME in the range 5.3–6.8 ppm. The corrected integrals for resonances corresponding to individual metabolites or the sums of integrals for all resonances assigned to a particular metabolite class (i.e. three phosphates for NTP, two for NDP, 3–4 PME resonances, etc.) were expressed as percentages of the total ^{31}P integral (minimum detectable integrals for PDE: ca. 0.5% of total P), omitting the integral for the narrow P_i(ext) resonance assigned to residual extracellular phosphate. These percentages were used as measures of relative metabolite concentrations in the subsequent analysis.

There are two main limitations in this type of analysis. First, a number of individual signal integrals determined by deconvolution of a broad multicomponent lineshape will be interdependent. For example, for the various PME components other than PC in the range 6.5–8 ppm, only the sum will be considered (PE + other PME); NTPγ and NDPβ overlap near −3 ppm; NDPN(α, β) and NDP-Hex(α) overlap at −8 ppm. Thus, for the calculation of individual metabolite levels, in particular for the various nucleotide types, sums and differences of integrals must also be computed. The second limitation is the scaling of the results as % tot. P. This implicitly assumes that the total concentration of all phosphates is a constant, which may not be true. Thus, a relative increase in one or more metabolites will automatically result in a decrease in the percentages calculated for all other metabolites. This problem of scaling is avoided when dimensionless metabolite ratios are examined.

Intra- and extracellular pH values were determined based on the chemical shifts of the resolved intra- and extracellular P_i signals, respectively, according to the calibration curve of Eq. (2):

$$\mathrm{pH} = 6.66 + \log \frac{\delta(\mathrm{Pi}) - 3.35}{5.63 - \delta(\mathrm{Pi})}, \quad (2)$$

which we determined for a reference buffer by measuring pH at 22°C and the chemical shift δ(Pi) at 4°C.

A bioenergetic status parameter *ES* [38] and a phosphorylation potential *PP* [39] were calculated from the total signal integrals S as shown in Eqs. (3 and 4) (square brackets indicate molar concentrations). Normally these quantities are expressed in terms of adenylate nucleotide concentrations (ATP, ADP); however, we have used total NTP and NDP in these formulas since only these quantities can be determined by ^{31}P-NMR of intact cells.

$$\text{Energy status: } ES = ([\mathrm{PCr}] + [\mathrm{NTP}])/[\mathrm{P_i}] = \{S(\mathrm{PCr}) + 0.333S(\mathrm{NTP})\}/S(\mathrm{P_i}) \quad (3)$$

$$\text{Phosphorylation potential: } PP = [\mathrm{NTP}]/([\mathrm{NDP}][\mathrm{P_i}]) = 0.333S(\mathrm{NTP})/\{0.5S(\mathrm{NDP})S(\mathrm{P_i})\} \quad (4)$$

Statistics

Statistical analysis was performed using the software package StatView (version 5.0.1) from the SAS Institute (Cary, NC, USA). ANOVA was employed to analyze for treatment effects with the null hypothesis that there is no difference in cell survival (Series 1) or phosphate metabolite concentrations or ratios (Series 2) between treatment and control groups. For Series 1 data the Dunnett multiple-comparison post-hoc test at significance level α = 0.05 was used to compare individual treatment group means to a common control group mean. Dunnett's test requires neither homogeneity of variances nor equal group sizes and takes into account the type I error probability for a set of $k-1$ comparisons to a single control group [40]. For simple comparisons of means, either the unpaired or paired t-test (two-sided, equal variance) was used as noted. Linear correlations between parameters were examined in terms of the Pearson correlation coefficient r and tested for significance with Fisher's r to z transformation. Nonparametric correlations were examined using the Spearman rank correlation coefficient ρ.

Results

Normal growth characteristics of KTCTL-2 and KTCTL-26 cells

KTCTL-2 is a poorly differentiated RCC that displays a polygonal morphology in culture. KTCTL-26 is more highly differentiated, with a large cytoplasm-to-nucleus ratio. The growth curves in Fig. 1 show that in our standard RPMI 1640 medium KTCTL-2 cells grow more rapidly (doubling time 23 h) than KTCTL-26 cells (doubling time 35 h) and continue to grow beyond confluence, piling up in multilayers. The characteristics of these two cell lines

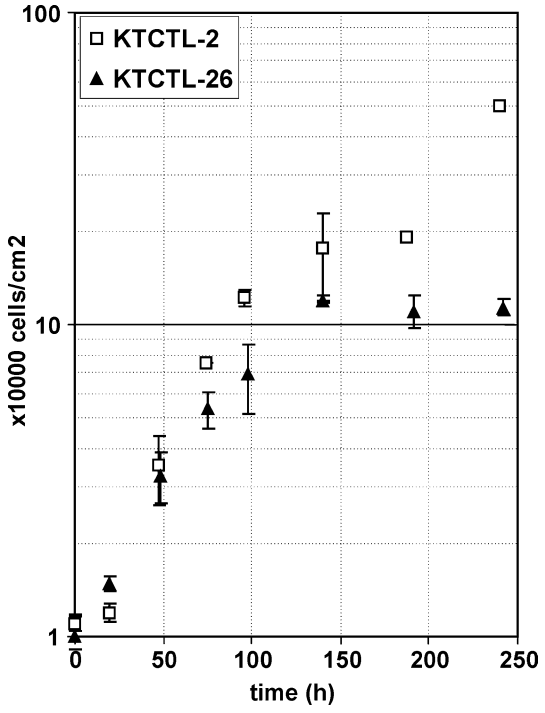

Fig. 1 Control growth curves ($\log_{10}$ cell density versus time) for the KTCTL-2 (low P-170) and KTCTL-26 (high P-170) human RCC lines in standard RPMI 1640 growth medium. Seeding density was 10^4 cells/cm^2. Symbols and error bars represent mean ± standard deviation for $n = 3$ determinations

are compared in Table 1. On the basis of a semiquantitative immuno-assay, KTCTL-2 and KTCTL-26 lines were found to express P-170 glycoprotein at relatively low and at moderately high levels, respectively (see Methods).

Treatment Series 1 (cell survival)

VBL treatment

The results of cell survival assays for KTCTL-2 or KTCTL-26 following 40 h incubations with VBL alone (Group 1B, Table 2) or with control medium are shown in Fig. 2a. Both cell lines exhibited a dose-dependent decrease in survival with increasing VBL (ANOVA for treatment effect, $p < 0.0001$), with KTCTL-26 showing a higher sensitivity to VBL. At the lowest VBL dose (0.011 μM) KTCTL-2 showed no effect of VBL (survival: 101.9 ± 4.9%) while KTCTL-26 showed a statistically significant decrease in survival (87.3 ± 9.5% vs. controls) according to Dunnett's test ($\alpha = 0.05$). At the highest VBL dose (11 μM) cell survival decreased to 62.8 ± 3.1% ($n = 3$) for KTCTL-2 cells and 43.7% ($n = 1$) for KTCTL-26 cells. Statistical significance of the effect of VBL on cell survival was achieved for both cell lines at the 0.11 μM or higher doses (Dunnett's test).

VBL + DIL treatment

In further experiments (Group 1C, Table 2) 40 h incubations were carried out with two concentrations of VBL and three concentrations of DIL. Figure 2b shows that the resistance of KTCTL-26 cells to 0.011 μM VBL was partially reversed by 1 or 10 μM DIL (bars with double asterisks) but not by 0.1 μM DIL. In contrast, the resistance of KTCTL-2 cells to 0.011 μM VBL could be reversed by DIL only at the 10 μM concentration. The statistical significance of resistance reversal was determined using multiple comparisons and Dunnett's test (see Methods).

Control incubations with DIL alone (group 1A, Table 2) showed no significant effects on cell survival at concentrations up to 10 μM. At 100 μM DIL direct toxicity was observed for KTCTL-26 cultures (78.2 ± 7.2% survival, data not shown), and this highest dose was not used in the comparative studies presented here.

Figure 2c shows analogous data for incubations with 1.1 μM VBL where significant cell kill was achieved without DIL. For KTCTL-26 a modest decrease in survival was observed with increasing DIL and became significant at 10 μM DIL. For KTCTL-2, which was more resistant to 1.1 μM VBL, no significant decrease in survival was observed when DIL was added at concentrations up to 10 μM.

IFN-α2b treatment

We previously reported that treatment with 10000 U/ml IFN-α2b alone resulted in a very *late* effect on cell survival (ca. 112% at 48 h, 55% at 96 h after treatment) for KTCTL-2 cells. The KTCTL-26 cell line was more sensitive to IFN-α2b; cell survival was only about 59% at 48 h and 28% at 96 h after treatment [32]. For comparison, in the current study with 40 h incubations, IFN-α2b at 10000 U/ml resulted in 113 ± 13% survival for KTCTL-2 and 99 ± 3% for KTCTL-26 (group 1H, Table 2).

Since IFN-α is frequently used in combination with VBL in the clinic [41,42], we were interested in the possible *early* effects of incubations employing IFN-α together with various combinations of VBL and DIL. Thus, a systematic study was carried out with the KTCTL-2 cell line: 40 h incubations analogous to those in Figs. 2b and 2c with 0–1.1 μM VBL and 0–10 μM DIL in the presence of 2000 U/ml IFN-α2b (groups 1D–1G, Table 2), i.e. at a more clinically relevant IFN-α dose than the 10000 U/ml used previously [32]. As expected, treatment with 2000 U/ml IFN-α2b *alone* had little effect on KTCTL-2 survival (93.7 ± 4.6% vs. untreated controls, Fig. 3). In the absence of VBL, increasing concentrations of DIL led to a trend toward an increase in survival (first group of bars in Fig. 3, one-way ANOVA for DIL effect: $p = 0.5634$). However, compared to Fig. 2b (no IFN), the presence of IFN-α2b made KTCTL-2 cells more sensitive

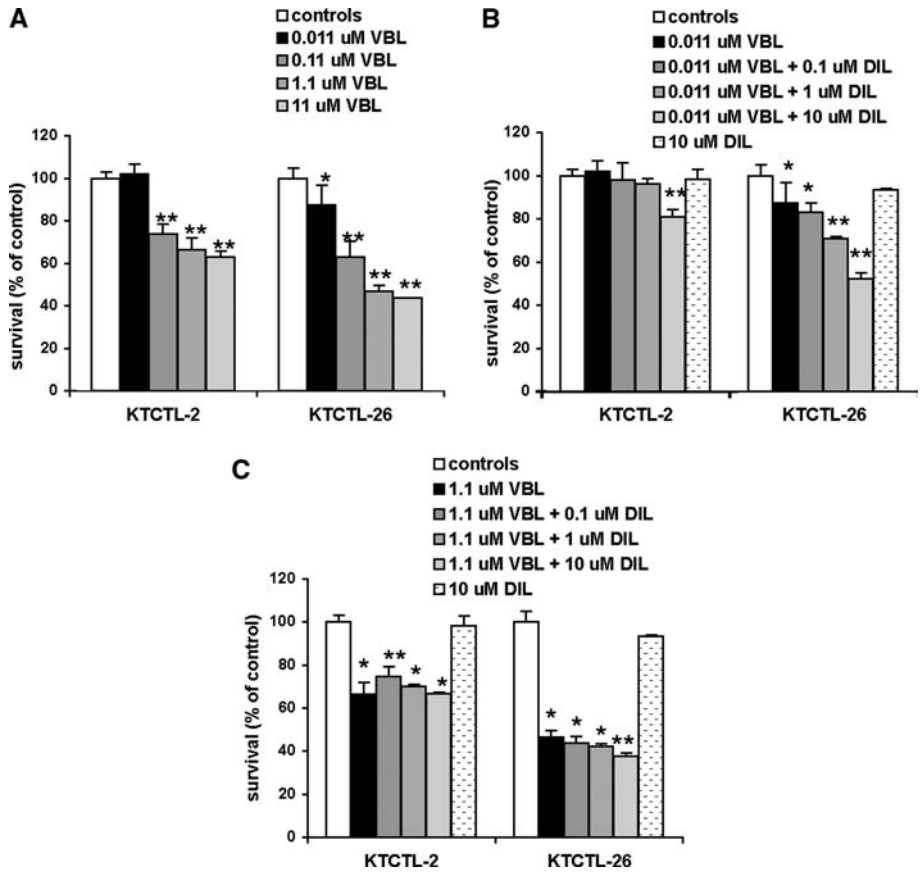

Fig. 2 Results of MTT cell survival assays (expressed as % of untreated controls) for cultured KTCTL-2 and KTCTL-26 cells after 40 h treatment with various concentrations of VBL and DIL. The legend for each pair of bar graphs indicates the drug concentrations used (*bars ordered from left to right*). **a** Treatment with VBL alone, 0–11 μM; **b** Treatment with 0.011 μM VBL and 0.1–10 μM DIL, or with 10 μM DIL alone; **c** Treatment with 1.1 μM VBL and 0.1–10 μM DIL, or with 10 μM DIL alone. Means ± standard deviations are shown for $n = 3$ except in the following cases: KTCTL-2 controls ($n = 4$), KTCTL-2 treated with 1.1 μM VBL alone or 0.011 μM VBL+ 10 μM DIL ($n = 2$), KTCTL-26 treated with 11 μM VBL alone ($n = 1$). Single asterisks indicate significant differences ($p < 0.05$) versus the corresponding controls (*white bars*). Double asterisks indicate significant differences versus controls *and* versus treatment with VBL alone in each group (*solid black bars*)

to reversal of resistance to 0.011 μM VBL treatment when DIL was present at 1 or 10 μM (82.9 ± 2.1% and 75.0 ± 5.3% survival, respectively; second group of bars in Fig. 3).

At the highest dose of VBL alone (1.1 μM), KTCTL-2 survival was about the same with or without IFN-α2b (70.9 ± 4.3% in Fig. 3, 66.4 ± 5.4% in Fig. 2c). In the presence of IFN-α2b (fourth set of bars in Fig. 3), but not in its absence (Fig. 2c), increasing DIL concentrations led to a significant dose-dependent *increase* in survival (from 70.9 ± 4.3% to 85.4 ± 0.8%; one-way ANOVA: $p = 0.0158$).

At the intermediate concentration of 0.11 μM VBL, there was no significant influence of IFN-α2b alone on KTCTL-2 survival (comparative data not shown). In the presence of IFN-α2b, the effect of DIL was not uniformly dose-dependent and can best be described as intermediate between the contrasting behaviors observed at lower and higher VBL concentrations (Fig. 3).

Summary

The survival assay data of Figs. 2 and 3 lead to the following observations and conclusions when the two RCC cell lines under study are compared.

(a) KTCTL-2 cells (more rapid growth, lower P-170 expression) are insensitive to 0.011 μM VBL alone and less sensitive to higher VBL concentrations than KTCTL-26 (slower growth, higher P-170 expression).
(b) For 40 h incubations the effect of VBL appears to saturate at concentrations approaching 10 μM; the minimum % survival reaches a plateau of ca. 63% for KTCTL-2 and 44% for KTCTL-26.
(c) At 0.011 μM VBL KTCTL-2 shows no response and the addition of DIL up to 1 μM also has no effect on survival; only at 10 μM DIL is a modest effect observed (81% survival).

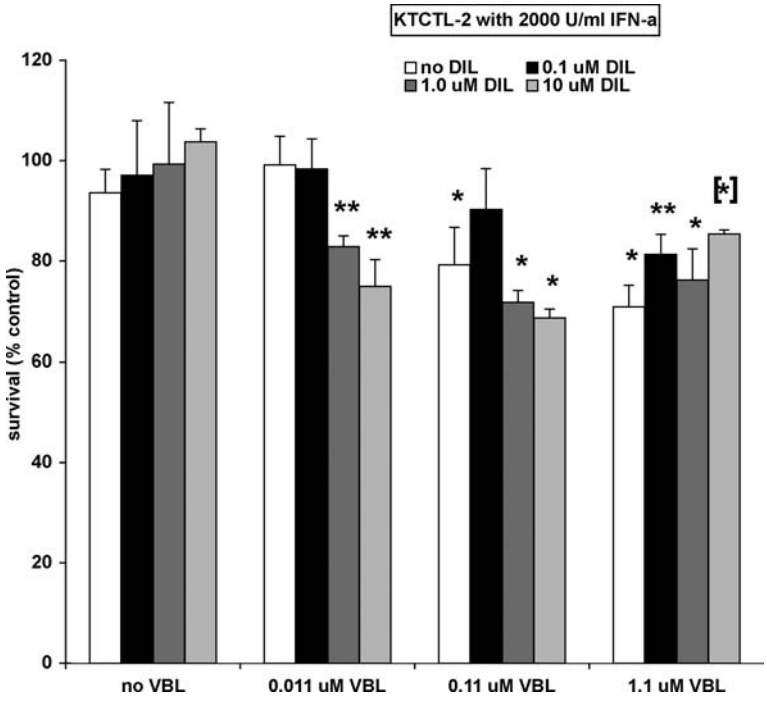

Fig. 3 MTT cell survival assays (as % of untreated controls) for cultured KTCTL-2 cells after 40 h treatment with 2000 U/ml IFN-α2b and various VBL/DIL combinations (analogous to Fig. 2). Means $\pm$ standard deviations are shown for $n = 3$. Single asterisks indicate significant differences ($p < 0.05$) versus untreated controls (100 $\pm$ 13%). Double asterisks indicate significant differences versus untreated controls and versus the corresponding VBL group with 0 DIL (*white bars*). A bracketed asterisk [*] denotes a VBL/DIL combination treatment that exhibited a significant difference versus the corresponding DIL = 0 treatment but *not* versus untreated controls

(d) KTCTL-26 responds weakly to 0.011 μ M VBL (87% survival) and shows a progressive dose-dependent decrease in survival with increasing DIL, reaching 52% survival at 10 μM DIL.
(e) At the high dose of 1.1 μM VBL, where the treatment effect for both cell lines is nearly saturated, the addition of DIL up to 10 μM has no effect for KTCTL-2 but leads to a small dose-dependent decrease in survival for KTCTL-26 (44–38%).
(f) Ten micromolar meter DIL alone has no effect on KTCTL-2 and only a minor effect on KTCTL-26 (93% survival).
(g) At 0.011 μM VBL the reversal of resistance by DIL was enhanced by IFN-α2b at DIL concentrations of 1 μM (83% vs. 96% survival without IFN-α2b) and 10 μM (75% vs. 81% survival).
(h) At 0.11 μM VBL in the presence of IFN-α2b, the addition of 0.1 μM DIL resulted in an *increase* in cell survival while 1 and 10 μM DIL caused a decrease in survival. For incubations without IFN-α2b, the addition of 0.1 μM DIL resulted in a modest increase in cell survival (from 74% to 81%) while 10 μM DIL caused a minor decrease in survival (to 65%); the addition of 1 μM DIL had virtually no effect on survival (75%; data not presented in Fig. 3).
(i) At 1.1 μM VBL in the presence of IFN-α2b, all three concentrations of DIL resulted in an *increase* in cell survival with a dose-dependent trend that was not observed in the absence of IFN-α2b. Survival at 10 μM DIL was 85% with IFN-α2b and 67% without.

Treatment Series 2 (phosphate metabolism)

Phosphate metabolite profiles in untreated cells

Examples of the ^{31}P NMR spectra obtained from control cell suspensions are shown in Fig. 4. Both cell lines exhibited an intracellular pH of 7.5–7.6, as determined on the basis of the chemical shift of the broad intracellular P_i signal at ca. 5.4 ppm (see below), which could be resolved from the narrow extracellular P_i signal at 5.15 ppm (buffer pH = 7.2). Thus, our results are consistent with other reports of alkaline intracellular tumor pH [19]. Most notable in the ^{31}P spectra for KTCTL-2, for example, was the near absence of phosphodiesters (<0.5%) and the clearly detectable signal for NDPβ.

Differences between the two cell lines in the relative levels of specific metabolites can be seen in the data summarized in Fig. 5 for untreated control cultures corresponding to three different experiments (cell batches). Table 3 summarizes the ^{31}P signal integral data for those metabolites that exhibited statistically significant

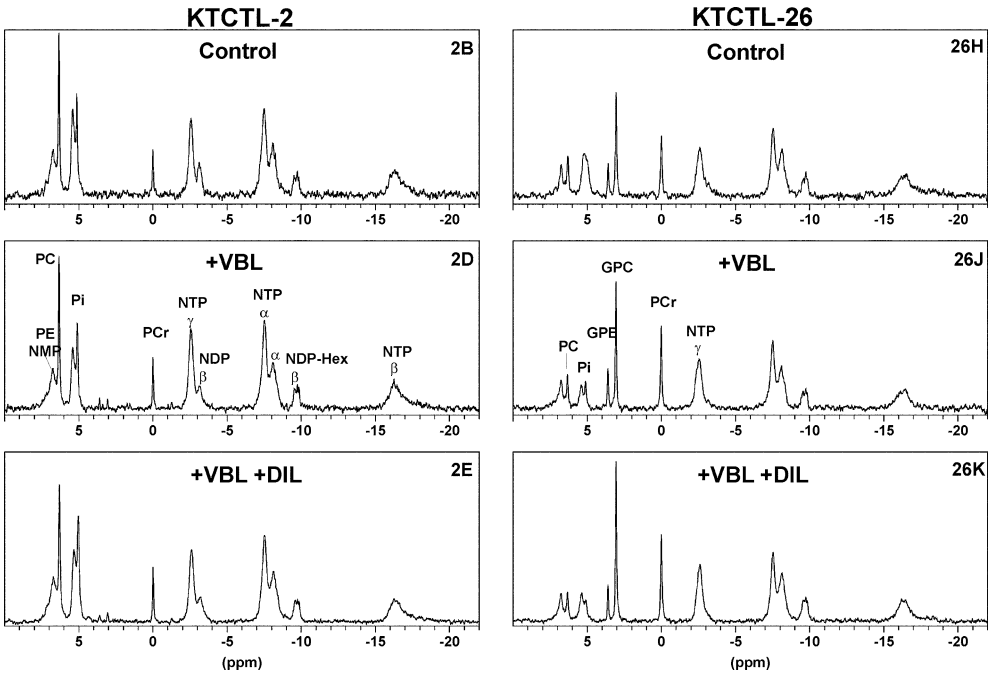

Fig. 4 202 MHz ^{31}P-NMR spectra of RCC cell suspensions at 4°C, comparing KTCTL-2 (*left*) and KTCTL-26 (*right*) as untreated controls (*top*), after 40 h treatment with 0.011 μM VBL alone (*center*), or after 40 h treatment with 0.011 μM VBL in combination with 10 μM DIL (*bottom*). For each sample cell numbers were in the range 4–8 $\times 10^7$, and the spectra represent 1800 transients acquired in 1 h with inverse-gated ^{1}H decoupling; 8 Hz linebroadening was applied before FT. For each cell line the vertical scale for each plotted spectra was adjusted to give the same peak area for NTPγ + NDPβ. The S/N in each spectrum thus reflects the cell count in the suspension. Resolved peaks are labeled according to the corresponding metabolites (see Abbreviations list). The broad peak at ca. 6.8 ppm represents primarily NMP with smaller contributions from PE as well as sugar phosphates and triose phosphates (δ_P = 7–8 ppm); the nucleotide peaks at −7.5 and −8.1 ppm also contain NDPα, NDPNα, β, respectively. The phosphate resonance for P_i is split into a broad and a narrow peak arising, respectively, from intracellular and extracellular P_i with chemical shifts corresponding to pH values of ca. 7.6 and 7.2, respectively

differences ($p < 0.015$) in relative concentrations for the two cell lines. In KTCTL-2 cells ($n = 5$) the levels of the phosphodiesters GPC (3.06 ppm) and GPE (3.60 ppm) were significantly lower than in KTCTL-26 cells (n = 6), while the levels of PC (6.35 ppm) were higher. Total PME was also higher for KTCTL-2, mainly due to the difference in PC levels. However, in KTCTL-2 there were also higher levels of the metabolites contributing to the broad resonance centered at ca. 6.8 ppm with shoulders in the range 7–7.8 ppm (PE + other = PE, NMP, sugar phosphates, and triose phosphates: 11.3 ± 1.7% vs. 9.7 ± 1.7%). Thus, the phospholipid metabolite *ratios*, PC/GPC and PME/PDE, which are widely considered to be indicators of cell growth [43], were more than 10 times higher for the faster growing KTCTL-2 cell line. For comparison the *inverse* ratio GPC/PC is shown in Table 3 because of the zero or near-zero levels of PDE in the KTCTL-2 cultures examined.

In terms of energy-related metabolites, P_i and NDP were significantly higher in KTCTL-2 while phosphocreatine (PCr) was lower (Fig. 5, Table 3). For NTP, NDP-Hex and NDPN levels, no significant differences between cell lines were detected. Table 3 summarizes the values of cellular-energy parameters, *ES* and *PP* (see Materials and methods), for the control cultures of Fig. 5, and both parameters were significantly higher for the KTCTL-26 cell line.

The determination of NDP in KTCTL-2 cells by deconvolution of the two-component signal for NTPγ(−2.57 ppm) and NDPβ(−3.17 ppm) was straightforward. With strong Lorentz-Gauss resolution enhancement it was also possible to deconvolute NDPα as a shoulder (−7.31 ppm) on the NTPα peak (−7.54 ppm) (data not shown). For KTCTL-26 this technique was not always successful due to the very low levels of NDP present (<2%). Thus, for two of the six control samples used for Table 3, NDP could not be evaluated by deconvolution and a value of 1.0% was assumed for the calculation of a quasi lower limit for the phosphorylation potential.

Another technique that has been frequently used in the past to estimate NDP levels is to calculate the difference between the integrals for the signals at ca. −2.6 ppm (NTPγ + NDPβ) and −16.3 ppm (NTPβ). However, this method will not give dependable results for NDP levels below about 2% due to S/N limitations and the inherent uncertainties in baseline correction and integration. Furthermore, we have regularly found that for ^{31}P spectra of intact cells measured at 11.7 T and 4°C the NTP β signal is actually composed of two components: a

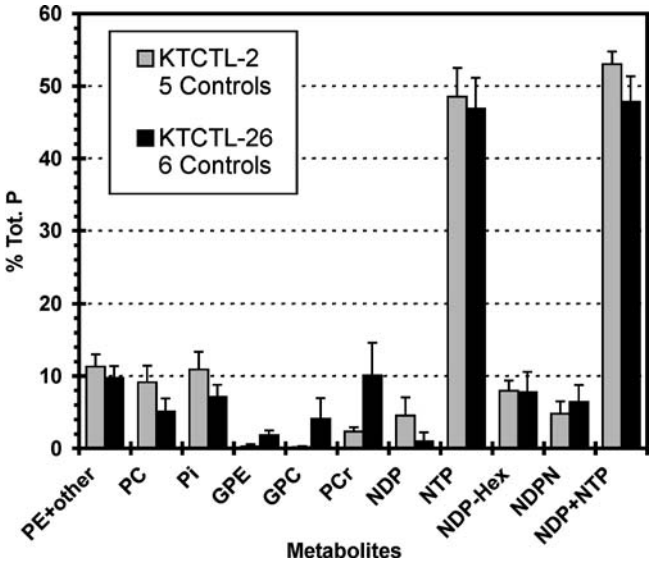

Fig. 5 Phosphate metabolite profiles are expressed here as *total* ^{31}P NMR signal integrals (mean ± SD as % of total phosphates) for the specified metabolite(s) for untreated, harvested KTCTL-2 ($n = 5$) and KTCTL-26 ($n = 6$) cell cultures (*controls*). Measurements were carried out on three separate occasions with different stock cultures and medium batches, leading to the relatively large SDs for some metabolites. Table 3 summarizes significant differences between the two cell lines

Table 3 Comparison of phosphate metabolite levels for cultured RCC cells, as determined by ^{31}P-NMR

Metabolites	^{31}P Signal Integral (% of total P) [a]	
	KTCTL-2 ($n = 5$)	KTCTL-26 ($n = 6$)
Total PME	20.5 ± 1.9	14.9 ± 2.6
PC	9.1 ± 2.3	5.1 ± 1.8
Pi(int)	10.9 ± 2.4	7.1 ± 1.7
GPE	0.30 ± 0.26	1.8 ± 0.7
GPC	0.17 ± 0.14	4.1 ± 2.8
PCr	2.3 ± 0.6	10.1 ± 4.5
NDP	4.5 ± 2.5	1.0 ± 1.3
NDP+NTP	53.1 ± 1.7	47.8 ± 3.5
Metabolite Ratios [b]		
GPC/PC	0.019 ± 0.013	0.98 ± 0.90
PDE/PME	0.023 ± 0.016	0.43 ± 0.30
ES	1.8 ± 0.6	4.0 ± 1.8
PP	0.6 ± 1.0	5.1 ± 3.7 [c]

[a] Mean ± SD of ^{31}P signal integrals for those metabolites that showed significant differences between the two cell lines ($p < 0.015$ in all cases, two-sided t-test, pooled variance); for all other evaluated metabolite signals, $p > 0.15$

[b] Energy status *ES* and phosphorylation potential *PP* were calculated as described in Methods; for all ratios differences between cell lines are significant with $p < 0.05$

[c] For 2 of 6 samples NDPβ was not detected; for the calculation NDP was set to 1.0% of tot. P (approximate detection threshold)

major signal at −16.3 ppm and broader minor component (ca. 10–20% of NTPβ) centered at ca. −17 to −18.5 ppm (visible in Fig. 4 as an asymmetry in the lineshape). Only when the integration is extended to cover −14 to −20 ppm, does the NTPβ integral approximately equal the integrals assigned to NTPα and NTPγ. The separation of the NTPβ signal into two components is due to the transition from a fast-exchange-averaged spectrum (obtained at lower field or higher temperature) to an intermediate-to-slow exchange spectrum under our conditions. The exchange equilibria [44,45] involve species such as $MgNTP^{2-}$, $HMgNTP^{1-}$, $KNTP^{3-}$, $HKNTP^{2-}$, $HNTP^{3-}$, and NTP^{4-}. For ATP the Pβ chemical shift is 18.4 ppm for $KATP^{3-}$ and 19.6 ppm for $HKATP^{2-}$ versus 15.7 and 17.4 ppm for the Mg^{2+} complexes [45]. The pK_a for $HATP^{3-}$ is 6.96 and the k_{off} rate for $MgATP^{2-}$ is 1200 s^{-1} at 37°C [44]. Under our conditions the chemical shift difference $\Delta\delta$ for Mg^{2+} binding is ca. 2.5 ppm = 500 Hz, and we have the situation $k_{off} \sim \pi\Delta\delta$ for intermediate exchange at 37°C. At 4°C $k_{off} < \pi\Delta\delta$ should apply, which represents a slow-exchange situation in which the NTPβ peak may exhibit two components.

There was no significant difference between cell lines in the intracellular pH of the harvested control cell suspensions used for NMR ($pH_{int} = 7.52 \pm 0.17$ and 7.49 ± 0.13, for KTCTL-2 and KTCTL-26, respectively), and for both cell lines at 4°C the difference between intra- and extracellular pH was maintained during the NMR measurement ($pH_{ext} = 7.18 \pm 0.07$ and 7.17 ± 0.04, respectively).

A few pilot experiments were also performed with the RCC cell lines embedded in basement membrane gel and perfused with medium at 37°C for up to 3–4 days (data not shown). ^{31}P-NMR spectra of control cultures exhibited many of the same characteristic differences in phosphate metabolite levels between the two cell lines, as listed in Table 3. KTCTL-2 had higher total PME and higher PC but very low levels of PCr and PDE compared to KTCTL-26. However, in perfusion cultures the significant difference in NDP levels noted for flask cultures was not apparent. A resolved NDP peak for KTCTL-2 was not detected, and for both cell lines NDP estimates were generally <3%. After a few hours of perfusion (equilibration) metabolite levels for KTCTL-2 were relatively stable over a 4-day period. In contrast, for KTCTL-26 the initially high levels of PC (10%) and PCr (7%) decreased progressively to about 2 and 1.5%, respectively, after about 80 h of perfusion with recirculated medium while GPC remained constant.

VBL/DIL treatment

Fig. 4 shows examples of the ^{31}P NMR spectra obtained from the two RCC cell lines after a 40 h treatment with 0.011 μM VBL alone and in combination with 10 μM DIL (which gave the maximum DIL effect in the survival

studies). Quantitative results for these treatments ($n = 2$) and for a single treatment with 1.1 μM VBL alone are presented in Fig. 6. For each cell line two sets of treatment experiments with a matching control culture were performed on separate occasions using different seed stock and medium/serum batch. These controls are included in the larger group of controls used for Fig. 5. It should be mentioned that in all cases the spectra of treated cells correspond to the largely viable cells still attached to the culture flask and harvested at the end of the 40 h incubation.

For the more resistant KTCTL-2 cell line, treatment with 0.011 μM VBL alone had no effect on survival (Fig. 2) and very little effect on phosphate metabolite levels except for a 3% decrease in intracellular P_i (from 12.7 ± 0.8% to 9.7 ± 0.3% tot. P), a 1.8% decrease in NDP and a 3.3% increase in NTP. These effects correspond to an increase from 1.4 to 2.0 in the calculated *ES* ratio (Table 4, $p = 0.018$, paired t-test). There were no significant changes in phospholipid metabolite levels, the ratio GPC/PC, or *PP* (Table 4).

For the more sensitive KTCTL-26 cell line, treatment with 0.011 μM VBL alone led to a minor decrease in survival (88%, Fig. 2) which was reflected in a decrease in P_i(2.5%), and increase in *ES* (2.8 to 3.8), an increase in GPC (2.2%), and a significant increase in the GPC/PC ratio (from 2.1 to 3.0, $p = 0.02$, paired t-test).

For the combined treatment VBL/DIL = 0.011/10 μM, only a small decrease in survival was observed for KTCTL-2 cells (82%, Fig. 2), and the effect on the phosphate metabolite profile was minor. PC decreased by about 1% compared to VBL treatment alone, and the GPC/PC ratio increased from 0.021 to 0.043 (Table 4) while *ES* and *PP* were unchanged. The combined VBL/DIL treatment had a stronger effect on the more sensitive KTCTL-26 cell line (52% survival, Fig. 2). Relative to VBL treatment alone, the following changes in metabolite levels (as % tot. P) were observed: 0.9% decrease in PE + other PME, 0.9% decrease in PC, 2.2% increase in GPC, 3.4% decrease in NTP+NDP. Thus, the GPC/PC ratio increased to 5.3 for the combined treatment of KTCTL-26 cells (Table 4).

Phosphate metabolite profiles were also determined for one experiment with high-dose VBL treatment (1.1 μM) as shown in Fig. 6 and Table 4. Significantly reduced survival was observed for both cell lines according to Fig. 2 (66% for KTCTL-2, 38% for KTCTL-26), and the following changes in metabolite levels in % tot. P vs. controls were found for KTCTL-2 and -26, respectively: −3.2% and −4.1% in tot. PME, −2.6% and −2.3% in PC, +0.3% and +1.5% in GPC, −3.3% and −2.1% in Pi, +9.0% and −2.3% in NTP+NDP. Thus, the ratio GPC/PC increased to 0.067 for KTCTL-2 and 7.2 for KTCTL-26. For each cell line the *ES* ratio was higher than for controls but about the same as for other treatments.

Treatments with 10 μM DIL alone, which showed no significant effect on survival, were also examined by ^{31}P NMR (data not shown). For both cell lines changes in metabolite signal integrals were less than 3% vs. controls and there were no changes in GPC/PC.

Due to the good detectability of the NDPβ signal in all KTCTL-2 cultures (Fig. 4), it was possible to calculate *PP* with reasonable accuracy (Table 4). This was not the case for KTCTL-26 where NDP levels were low and difficult to determine by deconvolution (see above). For one series of treatments deconvolution gave NDP levels of 0.6–1.4% which led to calculated values for *PP* which decreased from 2.0 for the control to 0.7 for the 1.1 μM VBL treatment (second column of values for KTCTL-26 in Table 4). For the other series of samples (first column in Table 4), NDP could not be determined in 3 cases, and the estimates shown in parentheses (first column in Table 4) were calculated for NDP = 1.0% and may represent approximate lower limits. In any event the significant differences in NDP and *PP* between the two cell lines were clear and were not dramatically affected by any of the treatments employed.

In a pilot experiment KTCTL-26 cells were equilibrated for 24 h in perfusion culture and then perfused for 48 h with medium containing 1.1 μM VBL + 10 μM DIL (data not shown). The basic trends described above were observed: PC and total PME decreased progressively and GPC/PC increased while NTP+NDP and PCr remained relatively constant.

IFN−α2b treatment

KTCTL-2 and KTCTL-26 cells in flask culture were incubated for 40 h with 10000 U/ml IFN-α2b (Fig. 6, Table 4). This treatment led to a small increase in survival for KTCTL-2 cells (see Series 1 above) which may be related to the small increase in PC and other PME observed by NMR (Fig. 6). For KTCTL-26 there was no change in survival relative to controls and no change in PC levels. For both cell lines IFN-α2b treatment led to the same decrease in P_i vs. controls that was also observed for the other treatments. The parameters listed in Table 4 had values similar to those observed for controls and for the ineffective treatment with 0.011 μM VBL. Thus, the lack of a significant effect on survival (MTT assay) for the high-dose, 40 h IFN-α2b treatment is consistent with the absence of major effects on metabolite levels obtained from the ^{31}P spectra.

Pilot experiments with *perfused* cells revealed no major effects of IFN-α2b (10000 U/ml) over ca. 60 h for either cell line. A decrease in PC and roughly constant GPC over the 4-day perfusion was observed for both control and treatment experiments, and the effect was larger for KTCTL-26 (GPC/PC = 1–1.5 initially and ca. 5–9 after 48 h). The initially high levels of PCr in KTCTL-26

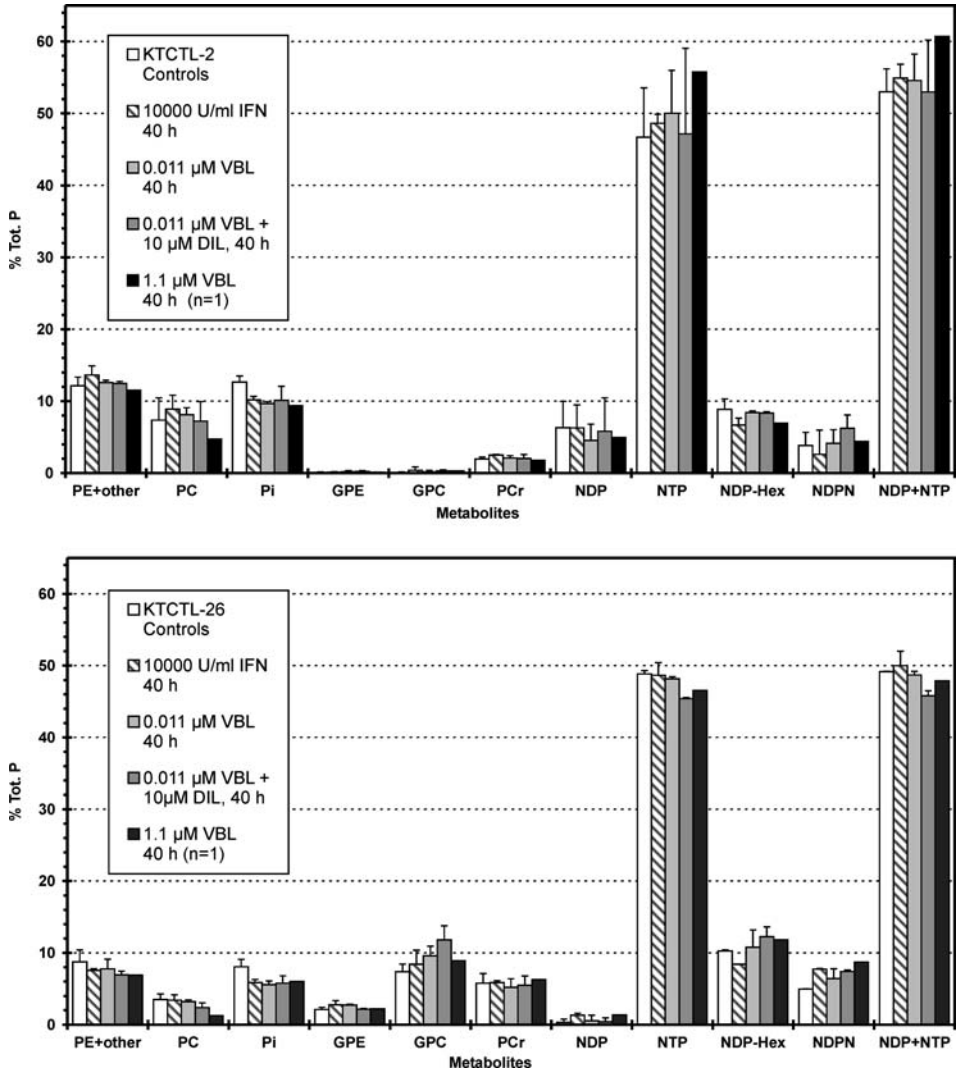

Fig. 6 Phosphate metabolite profiles based on ^{31}P NMR (as in Fig. 5) of KTCTL-2 (*top*) and KTCTL-26 (bottom) cell cultures harvested after various 40 h incubation treatments with IFN-α2b, VBL, and DIL (see legends). Means ± SDs are plotted for $n = 2$, except for 1.1 µM VBL alone ($n = 1$). For KTCTL-2 the levels of GPC and GPE were <0.5% in all cases

(7–11%) decreased to ca. 2% after 80 h of perfusion (control or IFN treatment) while the low PCr levels in KTCTL-2 (0.3–1.5%) remained in this range over the entire perfusion period.

Correlation of phosphate metabolite levels with treatment survival

In the treatment studies described above, it was evident that the relative levels of PC as % tot. P and the ratio GPC/PC were the most sensitive parameters for monitoring treatment effects. In Fig. 7 the differences (treatment minus control) for PC, PCr, PE + other PME (as % tot. P) and for the ratio GPC/PC as determined by NMR were plotted vs. the mean % survival figures (MTT assay) for five corresponding treatment protocols.

Nonparametric analysis of the pooled data for both cell lines gave Spearman rank correlation coefficients $\rho = 0.875$ ($p = 0.0086$) for PC versus % survival and $\rho = -0.778$ ($p = 0.020$) for GPC/PC versus % survival. Linear correlation analysis for the individual cell lines gave the following results for PC; KTCTL-2: $r = 0.950$, $p = 0.01$; KTCTL-26: $r = 0.904$, $p = 0.034$. Thus, for both cell lines PC appears to be a good indicator of treatment response. For KTCTL-26 the ratio GPC/PC was an even better indicator of response with $r = -0.985$, $p = 0.0005$ for all five treatments (with IFN treatment omitted: $r = -0.991$, $p = 0.007$). For KTCTL-2 the GPC/PC ratios were very low and difficult to measure, but a trend toward higher ratios with lower survival was observed ($r = -0.740$, $p = 0.18$, $n = 5$), in particular if the anomalous results (growth enhancement) of IFN treatment are omitted ($r = -0.998$, $p = 0.0004$, $n = 4$).

Table 4 Metabolic parameters for cultured RCC cells after various treatments, as determined by ^{31}P-NMR. [a]

	KTCTL-2	KTCTL-26
GPC/PC		
Control	0.013 ± 0.018	2.13 ± 0.17
10000 U/ml IFN	0.041 ± 0.043	2.61 ± 1.16
0.011 μM VBL	0.021 ± 0.022	2.97 ± 0.20 *
0.011 μM VBL + 10 μM DIL	0.043 ± 0.003	5.32 ± 2.34
1.1 μM VBL	0.067	7.15
Energy Status *ES*		
control [b]	1.39 ± 0.25	2.77 ± 0.54
10000 U/ml IFN	1.84 ± 0.04	3.77 ± 0.41 (*)
0.011 μM VBL	1.95 ± 0.23 *	3.83 ± 0.54
0.011 μM VBL + 10 μM DIL	1.83 ± 0.70	3.62 ± 0.42 (*)
1.1 μM VBL	2.17	3.62
Phosphorylation Potential *PP*		
control [b]	0.15 ± 0.09	(4.5)[c], 2.01
10000 U/ml IFN	0.21 ± 0.14	1.7, 1.7
0.011 μM VBL	0.25 ± 0.17	(5.4), 1.6
0.011 μM VBL + 10 μM DIL	0.26 ± 0.32	(6.0), 1.2
1.1 μM VBL	0.19	–, 0.7

[a] Mean ± SD for $n = 2$ for all treatments except 1.1 μM VBL ($n = 1$). An asterisk * denotes a significant difference between a treatment group and the corresponding control group (pairwise t-test, $p < 0.05$); (*) denotes $p = 0.06$

[b] A matched control culture was prepared from the same seed stock used for each of the two treatment series; these and other controls were used to prepare Table 3

[c] KTCTL-26: NDP could not be resolved by deconvolution for all samples; numbers in () represent lower bounds that were calculated assuming NDP = 1.0% tot. P (approximate detection threshold)

PE + other PME was not a good indicator for either cell line ($r < 0.8$), and changes in PCr were less than 1% for all treatments.

Discussion

Effects of VBL and DIL on RCC cell survival

Our results show that KTCTL-2 has significantly higher resistance to VBL despite its lower expression of P-170 (MDR1). The resistance to low-dose VBL treatment can only be partially reversed by high DIL. Thus, some other, highly efficient, non-P-170 resistance mechanism must be operating for KTCTL-2. On the other hand, KTCTL-26 exhibits higher P-170 expression but an overall lower resistance to VBL, which is more readily reversed by DIL. Thus, it appears that the primary (but less efficient) resistance mechanism for KTCTL-26 involves P-170.

The saturation of the VBL effect at high doses suggests that longer incubation times would be required to obtain more complete cell kill. However, similar experiments in which a total of 14 primary human RCC cell cultures were treated with doxorubicin, another MDR-susceptible drug, demonstrated the presence of saturation effects at high doses in ca. 50% of all samples, even after seven-day treatments [28]. The origin of this behavior remains to be determined.

Effects of IFN-α on KTCTL-2 response to VBL/DIL treatment

Based on data not shown, treatment of either RCC cell line with 100 U/ml IFN-α2b alone for 40 h resulted in no detectable change in cell growth (% survival). At a dose of 10000 U/ml there was no effect on KTCTL-26 cells while KTCTL-2 exhibited a minor growth enhancement similar to that observed previously [32] for a 48 h incubation (ca. 112% survival). The previous work demonstrated that significant effects of IFN-α on survival were observed only for incubation times >48 h.

In the present study, the main and complex influence of IFN-α2b was observed in VBL/DIL cotreatments. Thus, in the presence of 2000 U/ml IFN-α2b, KTCTL-2 cells showed decreased survival (enhanced reversal of resistance) for VBL/DIL treatments of 0.011/1 μM and 0.011/10 μM. Analogous behavior has been observed in other studies: (1) IFN-α2b enhanced the reversal of MDR to vincristine by MRK-16, a P-glycoprotein antibody, in MDR1 retrovirus-infected HT29 colon adenocarcinoma [46]; (2) IFN-α increased the modulation of doxorubicin by verapamil, a calcium channel blocker, in the

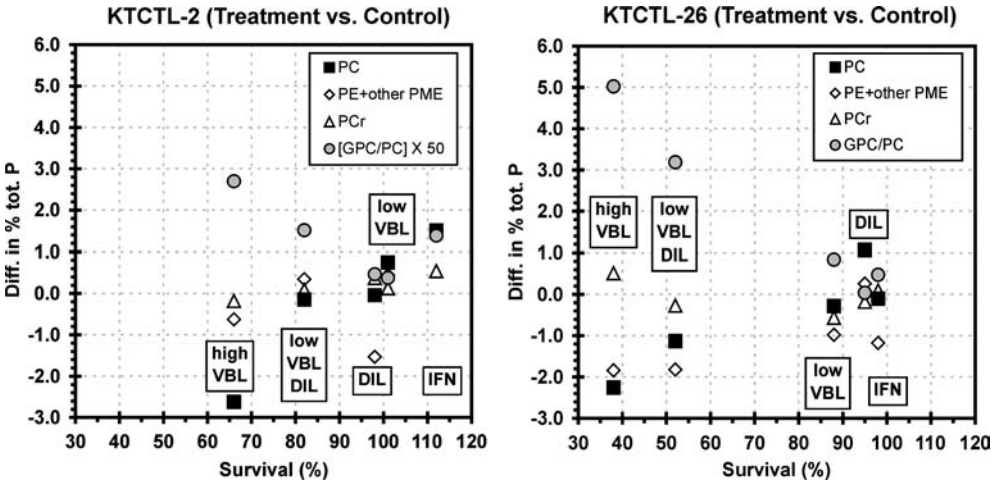

Fig. 7 Bivariate scatter plot for *changes* in key metabolite levels and the ratio GPC/PC (^{31}P NMR, Fig. 6) versus % survival (MTT assay, Fig. 2) under the same set of four treatment conditions. The treatment labels represent the following 40 h incubations relative to their matched controls: DIL = 10 μM DIL; low VBL = 0.011 μM VBL; low VBL DIL = 0.011 μM VBL + 10 μM DIL, high VBL = 1.1 μM VBL. The metabolite level or ratio data are the mean *differences* for treatment versus matched control for $n = 2$ experiments, except for high VBL (*both cell lines*) and DIL (KTCTL-2) where $n = 1$. The vertical numerical scale represents treatment-induced changes in % of Tot. P (metabolite levels) or in the dimensionless ratio GPC/PC (KTCTL-26) or GPC/PC multiplied by a factor 50 (KTCTL-2)

multidrug-resistant Chinese hamster ovary cell line MDR ChR C5 [47]; (3) IFN-α2b potentiated the doxorubicin sensitivity of the P-glycoprotein-positive colorectal carcinoma HCT-15 [48]. In our study the relatively moderate potentiation of the DIL effect by IFN-α2b in KTCTL-2 cells is consistent with our conclusion that the major contribution to resistance is by a non-P-170 mechanism.

Energetic status of untreated and treated KTCTL-2 and KTCTL-26 cells

Expression of the P-170 multidrug resistance phenotype often correlates with a more positive prognosis in RCC patients [49], since such tumors are generally more highly-differentiated [50], slower growing [50], and more responsive to combined chemotherapy and calcium antagonist treatment [28, 51] than undifferentiated tumors (e.g. KTCTL-2) that possess other, uncharacterized mechanisms of drug resistance. The high PCr levels found in KTCTL-26 cells (high P-170 expression) as opposed to KTCTL-2 cells (low P-170) are consistent with previously reported ^{31}P NMR studies of various *MDR1*-transfected cancer cells [20]. High PCr levels in cells which express P-170 may reflect an increased energy requirement for the operation of this membrane-bound pump [11, 20]. The higher PCr levels in KTCTL-26 may be useful in maintaining NTP levels during operation of the ATP-dependent P-170 efflux mechanism. In fact, Abraham et al. [52] discovered that P-170 serves as a channel for the steady release of ATP into the extracellular environment.

The lower energetic status of the KTCTL-2 cell line, in particular the lower PCr level, may be related to its lower expression of P-170. On the other hand, KTCTL-2 exhibited higher NDP + NTP levels which may be associated with its higher growth rate. Since this cell line exhibited a higher resistance to VBL/DIL treatments, other mechanisms of drug resistance [53] must be operative: e.g. via other members of the ATP-binding cassette (ABC) transporter family (MDR2/3), the multidrug resistance-associated protein MRP1 [54, 55], decreased activity of DNA topoisomerase IIα (atypical multidrug resistance, at-MDR), or increased Bcl-2 expression and inhibition of apoptosis [18, 56–58]. Thus, more specific experiments and more detailed determinations of protein expression levels will be necessary to elucidate the relative contributions of multiple resistance mechanisms to MDR in RCC. It has been noted elsewhere that the problem of multiple, redundant mechanisms of resistance has not been sufficiently appreciated in the MDR literature until recently [59]. While the two cell lines studied here exhibited significant differences in their normal complement of energy metabolites, in particular NDP, PCr, and P_i, treatment effects on the relative concentrations of these metabolites and the derived ratios were quite small and are poor indicators of treatment response.

Phospholipid metabolism in untreated KTCTL-2 and KTCTL-26 cells

PDE levels have been characterized for a variety of *MDR1*-transfected cancer cells [20] and a number of cancer cell lines rendered multidrug-resistant by selection with adriamycin [20, 60], actinomycin D [20] or mitoxantrone [25]. When compared with the corresponding

wild-type parental cells, the MDR variants exhibited significantly *lower* PDE levels, except for multidrug-resistant skin cancer cells (KB and FEM-X) which displayed *higher* PDE levels [20]. The former effect is in agreement with our finding that the more resistant KTCTL-2 cell line exhibited significantly lower PDE levels than the less resistant KTCTL-26. However, our results and those in the literature are difficult to interpret without more detailed knowledge of the relative contributions of P-170 and other mechanisms to MDR in the cell lines studied.

In fact, a large body of work indicates that MDR is associated with marked changes in membrane lipid composition [61]. More specifically, phosphatidylserine and phosphatidylethanolamine appear to be associated with the P-170 molecule, and adequate lipidation is essential for the P-170-associated ATPase activity [62]. In this context, the enhanced GPE levels found in KTCTL-26 vs. KTCTL-2 cells would be in agreement with the need for increased phosphatidylethanolamine turnover.

PC and GPC/PC as indicators of treatment response

The results summarized in Figs. 6 and 7 and Table 4 and the corresponding correlation analysis indicate that the relative concentration of PC can serve as a sensitive indicator of treatment effects for the two RCC cell lines investigated in this study. This correlation is also consistent with the growth enhancement and increase in PC observed for IFN treatment of KTCTL-2 cells.

Even better correlations with % survival are obtained for the ratio GPC/PC for both cell lines when the apparently anomalous data for IFN treatment are discarded. The decrease in PC and increase in GPC/PC that we observed in association with reduced survival may be explained in part by increased membrane catabolism via phospholipase A_2 as observed by Ruiz-Cabello et al. [63] and/or cell growth arrest. A decrease in PME has been frequently reported as an indicator for tumor response to therapy [19, 43, 64, 65]. Our results are consistent with this observation, whereby the decrease in total PME is primarily due to the decrease in PC.

Alterations in PME and PDE levels in KTCTL-26 cells following treatment could also be caused by operation of the P-170 mechanism. If the activation of P-glycoprotein-mediated drug export following VBL addition results in an increase in the rate of membrane turnover and changes in membrane structure, the observed steady-state levels of PME and PDE may also change. However, treatment with low VBL + DIL (inhibition of P-170) resulted in larger changes in GPC/PC than those observed after treatment with low VBL alone (P-170 active), indicating that GPC/PC is more closely related to cell growth than to P-170 activity.

Conclusion

A close relationship between cellular P-170 expression, energy-dependent transport processes and multidrug resistance is now well established. This provides a rationale for modulation of vinblastine and other drug treatments by calcium antagonists. Based on this knowledge, we conclude that the observed differences in energy metabolite profiles for the two RCC cell lines examined here are related to their different levels of P-170 expression, providing further corroboration for the basic mechanism of P-170-mediated MDR.

The complex interactions between *phospholipid metabolism*, energy-dependent phospholipid flipping, P-glycoprotein multidrug transport and modulated (or unmodulated) MDR are still under investigation [66–70]. Here, we have shown that therapy response and phospholipid metabolite parameters (PC, GPC/PC) are correlated for the RCC lines investigated. However, this correlation is most likely the result of basic cell biochemistry rather than specific MDR- or P-170-related mechanisms.

The effects of cytokines such as IFN-α on multidrug-resistant cells and the modulation of cytotoxic drugs by cytokines appear to be rather complex topics. Synergistic or potentiating effects have been reported for drug combinations in different cancer cell lines, in the presence or absence of calcium antagonists, for IFN-α [46–48] or other cytokines such as IFN-γ, TNF-α and IL-2 [71, 72]. Further elucidation of the underlying mechanisms is necessary to efficiently optimize these treatment modes, which are presently being tested in the clinic for kidney tumors [2, 41, 42, 53, 73, 74] and for other cancers [75] (for a review, see Ling [76]). Among the currently used immunochemotherapeutic treatment regimens, the combination of IFN-α with VBL can be considered as well-established [1]. However, with cytokine therapy the possibility of wide-ranging systemic side effects must be taken into account. The results presented here should provide useful baseline information for future in-vivo ^{31}P NMR studies to be carried out with experimental animals and patients.

Acknowledgements We are grateful to Dr. G. Fürstenberger for providing cell culture facilities. We kindly thank Dr. E. Pommerenke and Professor M. Volm of the Institute of Experimental Pathology at the German Cancer Research Center for performing the assays of P-170 glycoprotein, vimentin, and cytokeratin 18 expression.

References

1. Griniatsos J, Michail PO, Menenakos C, Hatzianastasiou D, Koufos C, Bastounis E (2003) Metastatic renal clear cell carcinoma mimicking stage IV lung cancer. Intl Urol Nephrol 35:15–17
2. Bichler K-H, Wechsel HW (1999) The problematic nature of metastasized renal cell carcinoma. Anticancer Res 19:1463–1466
3. Bak M, Efferth T, Mickisch G, Mattern J, Volm M (1990) Detection of drug resistance and P-glycoprotein in human renal cell carcinomas. Eur Urol 17:72–75
4. Kakehi Y, Kanamaru H, Yoshida O, Ohkubo H, Nakanishi S, Gottesman MM, Pastan I (1988) Measurement of multidrug-resistance messenger RNA in urogenital cancers; elevated expression in renal cell carcinoma is associated with intrinsic drug resistance. J Urol 139:862–865
5. Chabner BA, Fojo A (1989) Multidrug resistance: P-glycoprotein and its allies-the elusive foes. J Natl Cancer Inst 81:910–913
6. Mickisch GH (1993) Current status and future directions of research on multidrug resistance. The impact of contemporary biotechnology. Urol Res 21:79–81
7. Rothenberg M, Ling V (1989) Multidrug resistance: molecular biology and clinical relevance. J Natl Cancer Inst 81:907–910
8. Naito M, Tsuruo T (1989) Competitive inhibition by verapamil of ATP-dependent high affinity vincristine binding to the plasma membrane of multidrug-resistant K562 cells without calcium ion involvement. Cancer Res 49:1452–1455
9. Dalton WS, Sikic BI (1994) The multidrug resistance gene (MDR1) represents a potential target for reversing drug resistance in human malignancies. J NIH Res 6:54–58
10. Pastan I, Gottesman MM (1991) Multidrug resistance. Annu Rev Med 42:277–286
11. Horio M, Gottesman MM, Pastan I (1988) ATP-dependent transport of vinblastine in vesicles from human multidrug-resistant cells. Proc Natl Acad Sci USA 85:3580–3584
12. Mickisch GH, Roehrich K, Koessig J, Forster S, Tschada RK, Alken PM (1990) Mechanisms and modulation of multidrug resistance in primary human renal cell carcinoma. J Urol 144:755–759
13. Naito S, Koike K, Ono M, Machida T, Tasaka S, Kiue A, Koga H, Kumazawa J (1998) Development of novel reversal agents, imidazothiazole derivatives, targeting MDR1-and MRP-mediated multidrug resistance. Oncology Res 10:123–132
14. Silverman JA (1999) Multidrug-resistance transporters: In: Amidon GL, Sadee W (eds) Membrane transporters as drug targets, vol 12. Kluwer Academic/Plenum Publishers, New York, pp 353–386
15. Ernest S, Bello-Reuss E (1998) P-glycoprotein functions and substrates: Possible roles of MDR1 gene in the kidney. Kidney Int 53:S11-S17
16. Higgins CF, Gottesman MM (1992) Is the multidrug transporter a flippase? Trends Biochem Sci 17:18–21
17. Van Helvoort A, Smith AJ, Sprong H, Fritzsche I, Schinkel AH, Borst P, Van Meer G (1996) MDR1 P-glycoprotein is a lipid translocase of broad specificity, while MDR3 P-glycoprotein specifically translocates phosphatidylcholine. Cell 87:507–517
18. Fojo T, Bates S (2003) Strategies for reversing drug resistance. Oncogene 22:7512–7523
19. Negendank WG (1992) Studies of human tumors by MRS: A review. NMR Biomed 5:303–324
20. Kaplan O, Jaroszewski JW, Clarke R, Fairchild CR, Schoenlein P, Goldenberg S, Gottesman MM, Cohen JS (1991) The multidrug resistance phenotype: 31P nuclear magnetic resonance characterization and 2-deoxyglucose toxicity. Cancer Res 51:1638–1644
21. Le Moyec L, Tatoud R, Degeorges A, Calabresse C, Bauza G, Eugène M, Calvo F (1996) Proton nuclear magnetic resonance spectroscopy reveals cellular lipids involved in resistance to adriamycine and taxol by the K562 leukemia cell line. Cancer Res 56:3461–3467
22. Le Moyec L, Legrand O, Larue V, Kawakami M, Marie J-P, Calvo F, Hantz E, Taillandier E (2000) Magnetic resonance spectroscopy of cellular lipid extracts from sensitive, resistent and reverting K562 cells and flow cytometry for investigating the P-glycoprotein function in resistance reversion. NMR Biomed 13:92–101
23. Mannechez A, Collet B, Payen L, Lecureur V, Fardel O, Le Moyec L, De Certaines J-D, Leray G (2001) Differentiation of the P-gp and MRP1 multidrug resistance systems by mobile lipid 1H-NMR spectroscopy and phosphatidylserine externalization. Anticancer Res 21:3915–3920
24. Santini MT, Romano R, Rainaldi G, Filippini P, Bravo E, Porcu L, Motta A, Calcabrini A, Meschini S, Indovina PL, Arancia (2001) The relationship between 1H-NMR mobile lipid intensity and cholesterol in two human tumor multidrug resistant cell lines (MCF-7 and LoVo). Biochim Biophys Acta 1531:111–131
25. Venkatesan PV, Saravanan K, Nagarajan B (1998) Characterization of multidrug resistance and monitoring of tumor response by combined 31P and 1H nuclear magnetic resonance spectroscopic analysis. Anti-Cancer Drugs 9:449–456
26. Vivi A, Tassini M, Ben-Horin H, Navon G, Kaplan O (1997) Comparison of action of the anti-neoplastic drug Ionidamine on drug-sensitive and drug-resistant human breast cancer cells: 31P and 13C nuclear magnetic resonance studies. Breast Cancer Res Treat 43:15–25
27. DeVita VT, Hellman S, Rosenberg SA (1997) Cancer, principles and practice of oncology, vol 1 Lippincott-Raven, Philadelphia New York
28. Efferth T, Dunn TA, Berlion M, Langenbahn H, Pommerenke EW, Volm M (1993) Reversal of inherent multidrug-resistance in primary human renal cell carcinoma cell cultures by S 9788. Anticancer Res 13:905–908
29. Efferth T, Lohrke H, Volm M (1990) Correlations between natural resistance to doxorubicin, proliferative activity, and expression of P-glycoprotein 170 in human kidney tumor cell lines. Urol Res 18:309–312
30. Efferth T, Lohrke H, Volm M (1989) Reciprocal correlation between expression of P-glycoprotein and accumulation of rhodamine 123 in human tumors. Anticancer Res 9:1633–1637
31. Mosman T (1983) Rapid colorimetric assay for cellular growth and survival: Application to proliferation and cytotoxicity assays. J Immunol Methods 65:55–63

32. Frank MH, Pomer S (1999) Interferon alpha2b differentially affects proliferation of two human renal cell carcinoma cell lines differing in the P-glycoprotein-associated multidrug-resistant phenotype. J Cancer Res Clin Oncol 125:117–120
33. Franks SE, Kuesel AC, Lutz NW, Hull WE (1996) 31P MRS of human tumor cells: Effects of culture media and conditions on phospholipid metabolite concentrations. Anticancer Res 16:1365–1374
34. Kuesel AC, Donnelly SM, Halliday W, Halliday GR, Sutherland GR, Smith ICP (1994) Mobile lipids and heterogeneity of brain tumours as detectable by *ex vivo* 1H MR specroscopy. NMR Biomed 7:172–180
35. Shedd SF, Lutz NW, Hull WE (1993) The influence of medium formulation on phosphomonoester and UDP-hexose levels in cultured human colon tumor cells as observed by 31P NMR spectroscopy. NMR Biomed 6:254–263
36. Lutz NW, Kuesel AC, Hull WE (1993) A 1H NMR method for determining temperature in cell culture perfusion systems. Magn Reson Med 29:113–118
37. Kuesel AC, Graschew G, Hull WE, Lorenz W, Thielmann HW (1990) 31P NMR studies of cultured human tumor cells Influence of pH on phospholipid metabolite levels and the detection of cytidine 5′-diphosphate choline. NMR Biomed 3:78–89
38. Rofstad EK, DeMuth P, Fenton BM, Sutherland RM (1988) 31P nuclear magnetic resonance spectroscopy studies of tumor energy metabolism and its relationship to intracapillary oxyhemoglobin saturation status and tumor hypoxia. Cancer Res 48:5440–5446
39. Stryer L (1995) Biochemistry, 4th edn. WH Freeman and Company, New York
40. StatView (1999) Reference book. SAS Institute, Cary
41. Huland E, Heinzer H, Timm S, Aalamian M, Huland H (2002) Immuntherapie des metastasierenden Nierenzellkarzinoms in Deutschland. Urologe (A) 41:282–287
42. Krug J, Fritzsch J, Aust G (1995) Induction of insulin antibodies and insulin allergy under alpha-interferon treatment of renal cell carcinoma in a patient with insulin-treated diabetes mellitus - a case report. Int Arch Allergy Immunol 106:169–172
43. Podo F (1999) Tumour phospholipid metabolism. NMR Biomed 12:413–439
44. Mulquiney PJ, Kuchel PW (1999) Using the beta/alpha peak-height ratio of ATP in 31P spectra to measure free [Mg2+]: theoretical and practical problems. NMR Biomed 12:217–220
45. Willcocks JP, Mulquiney PJ, Ellory JC, Veech RL, Radda GK, Clarke K (2002) Simultaneous determination of low free Mg2+ and pH in human sickle cells using 31P NMR spectroscopy. J Biol Chem 277:49911–49920
46. Fogler WE, Pearson JW, Volker K, Ariyoshi K, Watabe H, Riggs CW, Wiltrout RH, Longo DL (1995) Enhancement by recombinant human interferon alfa of the reversal of multidrug resistance by MRK-16 monoclonal antibody. J Natl Cancer Inst 87:94–104
47. Kang Y, Perry RR (1994) Effect of alpha-interferon on P-glycoprotein expression and function and on verapamil modulation of doxorubicin resistance. Cancer Res 54:2952–2958
48. Lucero Gritti MF, Beviacqua M, Bordenave RH, Rumi LS (2001) Interferon-alpha 2b modulation of doxorubicin sensitivity in a multidrug resistant cell line. J Exp Clin Res 20:393–400
49. Hofmockel G, Bassukas ID, Wittmann A, Dammrich J (1997) Is the expression of multidrug resistance gene product a prognostic indicator for the clinical outcome of patients with renal cancer? Br J Urol 80:11–17
50. Oudard S, Levalois C, Andrieu JM, Bougaran J, Validire P, Thiounn N, Poupon MF, Fourme E, Chevillard S (2002) Expression of genes involved in chemoresistance, proliferation and apoptosis in clinical samples of renal cell carcinoma and correlation with clinical outcome. Anticancer Res 22:121–128
51. Giaccone G, Pinedo HM (1996) Reversal of MDR in solid tumors: In: Gupta S, Tsuruo T (eds) Multidrug resistance in cancer cells. Wiley, Chichester, pp 473–491
52. Abraham EH, Prat AG, Gerweck L, Seneveratne T, Arceci RJ, Kramer R, Guidotti G, Cantiello HF (1993) The multidrug resistance (mdr1) gene product functions as an ATP channel. Proc Natl Acad Sci USA 90:312–316
53. Hartmann JT, Bokemeyer C (1999) Chemotherapy for renal cell carcinoma. Anticancer Res 19:1541–1544
54. Efferth T, Thelen P, Schulten HG, Bode ME, Granzen B, Beniers AJ, Mertens R, Ringert RH, Gefeller O, Jakse G, Fuzesi L (2001) Differential expression of the multidrug resistance-related protein MRP1 in the histological compartments of nephroblastomas. Int J Oncol 19:367–371
55. Gottesman MM, Fojo T, Bates SE (2002) Multidrug resistance in cancer: Role of ATP-dependent transporters. Nat Rev Cancer 2:48–58
56. Kellen JA (1995) Alternative mechanisms of multidrug resistance in cancer. Birkhaeuser, Boston
57. Scheltema JMW, Romijn JC, Van Steenbrugge GJ, Beck WT, Schroeder FH, Mickisch GH (1997) Decreased levels of topoisomerase IIa in human renal cell carcinoma lines resistant to etoposide. J Cancer Res Clin Oncol 123:546–554
58. Scheltema JMW, Romijn JC, Van Steenbruggev, Schroeder FH, Mickisch GH (2001) Inhibition of apoptotic proteins causes multidrug resistance in renal carcinoma cells. Anticancer Res 21:3161–3166
59. Sikic B, Fisher GA, Lum BL, Halsey J, Beketic-Oreskovic L, Chen G (1997) Modulation and prevention of multidrug resistance by inhibitors of P-glycoprotein. Cancer Chemother Pharmacol 40:S13-S19
60. Cohen JS, Lyon RC, Chen C, Faustino PJ, Batist G, Shoemaker M, Rubalcaba E, Cowan KH (1986) Differences in phosphate metabolite levels in drug-sensitive and -resistant human breast cancer cell lines determined by 31P magnetic resonance spectroscopy. Cancer Res 46:4087–4090
61. Lavie Y, Fiucci G, Czarny M, Liscovitch M (1999) Changes in membrane microdomains and caveolae constituents in multidrug-resistant cancer cells. Lipids 34:S57-S63
62. Sharom FJ (1997) The P-glycoprotein multidrug transporter: interactions with membrane lipids, and their modulation of activity. Biochem Soc Trans 25:1088–1096
63. Ruiz-Cabello J, Cohen JS (1992) Phospholipid metabolites as indicators of cancer cell function. NMR Biomed. 5:226–33
64. Evelhoch JL, Keller NA, Corbett TH (1987) Response-specific adriamycin sensitivity markers provided by in vivo 31P nuclear magnetic resonance spectroscopy in murine mammary adenocarcinomas. Cancer Res 47:3396–3401
65. Tausch-Treml R, Kopf-Maier P, Baumgart F, Gewiese B, Ziessow D, Scherer H, Wolf KJ (1991) 31P nuclear magnetic resonance spectroscopy, histology and cytokinetics of a xenografted hypopharynx carcinoma following treatment with cisplatin: Comparison in three sublines with increasing resistance. Br J Cancer 64:485–493

66. Castaing M, Brouant P, Loiseau A, Santelli-Rouvier C, Santelli M, Alibert-Franco S, Mahamoud A, Barbe J (2000) Membrane permeation by multidrug-resistance-modulators and non-modulators: Effects of hydrophobicity and electric charge. J Pharm Pharmacol 52:289–296
67. Lo Y-L (2000) Phospholipids as multidrug resistance modulators of the transport of epirubicin in human intestinal epithelial Caco-2 cell layers and everted gut sacs of rats. Biochem Pharmacol 60:1381–1390
68. Romsicki Y, Sharom FJ (2001) Phospholipid flippase activity of the reconsituted P-glycoprotein multidrug transporter. Biochemistry 40:6937–6947
69. Senchenkov A, Litvak DA, Cabot MC (2001) Targeting ceramide metabolism - a strategy for overcoming drug resistance. J Natl Cancer Inst 93:347–357
70. Zhou Y, Gottesman M, Pastan I (1999) Domain exchangeability between the multidrug transporter (MDR1) and phosphatidylcholine flippase (MDR2). Mol Pharmacol 56:997–1004
71. Stein U, Walther W, Shoemaker RH (1996) Modulation of mdr1 expression by cytokines in human colon carcinoma cells: an approach for reversal of multidrug resistance. Br J Cancer 74:1384–1391
72. Monti F, Lalli E, Bontadini A, Szymczuk S, Pini E, Tononi A, Fattori PP, Facchini A, Ravaioli A (1994) Synergism between gamma interferon and doxorubicin in a human MDR colon adenocarcinoma cell line. J Chemother 6:337–342
73. Basting R, Corvin S, Haendel D, Hinke A, Schmidt D (1999) Adjuvant immunotherapy in renal cell carcinoma – comparison of interferon alpha treatment with an untreated control. Anticancer Res 19:1545–1548
74. Buzogany I, Czvalinga I, Gotz F (1997) Results of ambulatory mono- and combined interferon therapy in advanced kidney tumors. Orv Hetil 138:67–70
75. Jelic S, Babovic N, Stamatovic L, Kreacic M, Matkovic S, Popov I (2001) Vinblastin-carboplatin for metastatic cutaneous melanoma as first-line chemotherapy and in dacarbazine failures. Med Oncol 18:189–195
76. Ling V (1997) Multidrug resistance: Molecular mechanisms and clinical relevance. Cancer Chemother Pharmacol 40:S3–S8
77. Data Sheet Dilzem, Medsafe, 2002 (www.medsafe.govt.nz/Datasheet-Page.htm)
78. Bennett CL, Vogelzang NJ, Ratain MJ, Reich SD (1986) Hyponatremia and other toxic effects during a phase I trial of recombinant human gamma interferon and vinblastine. Cancer Treat Rep 70:1081–1084
79. Gutterman JU, Fine S, Quesada J, Horning SJ, Levine JF, Alexanian R, Bernhardt L, Kramer M, Spiegel H, Colburn W, Trown P, Merigan T, Dziewanowski Z (1982) Recombinant leukocyte A interferon: Pharmacokinetics, single-dose tolerance, and biologic effects in cancer patients. Ann Intern Med 96:549–556
80. Nanus DM, Pfeffer LM, Bander NH, Bahri S, Albino AP (1990) Antiproliferative and antitumor effects of a-interferon in renal cell carcinomas: Correlation with the expression of a kidney-associated differentiation glycoprotein. Cancer Res 50:4190–4194